SURFACE AND INTERFACE ANALYSIS
Surf. Interface Anal. 2003; **35**: 491–495
Published online in Wiley InterScience (www.interscience.wiley.com). DOI: 10.1002/sia.1561

SIA

Quantitative SIMS analysis of SiC

Yu. Kudriavtsev,[1]* A. Villegas,[1] A. Godines,[1] R. Asomoza[1] and I. Usov[2]

[1] Dep. Ingenieria Electrica-SEES, CINVESTAV-IPN, Mexico D.F., Mexico
[2] Curriculum in Applied and Materials Sciences, University of North Carolina at Chapel Hill, NJ, USA

Received 4 November 2002; Revised 13 March 2003; Accepted 17 March 2003

We performed a systematic study of ion-implanted 6H-SiC standards to find the optimal regimes for SIMS analysis. Relative sensitivity factors (RSFs) were acquired for operating conditions typical of practical SIMS applications. The experimental SiC RSFs were compared with those found for silicon:[1] the matrix effect was insignificant in most cases. It was found that the SiO^- cluster ion cannot represent correctly the real oxygen distribution in SiC. The physics of the effect is discussed. Copyright © 2003 John Wiley & Sons, Ltd.

KEYWORDS: SIMS; ion implantation; SiC

INTRODUCTION

Secondary ion mass spectrometry (SIMS) is one of the best methods of elemental analysis of different materials due to its excellent sensitivity and high depth resolution. All these advantages become particularly apparent in the case of SIMS analysis of ion-implanted SiC, which has became the material of choice for high-frequency and high-power electronics.

The SIMS technique provides a semi-quantitative analysis and requires standards for quantitative analysis. A matrix effect makes it impossible to apply relative sensitivity factors (RSFs) obtained for one material for analysis of another material.

In this work we present systematic SIMS analysis data of implanted 6H-SiC standards for the elements H, Be, B, N, O and Al, which are widely used for the fabrication of electronic structures and devices. We looked for the best conditions for SIMS analysis of these elements and also investigated other analytical regimes. Experimental RSFs were collected in summary tables and were compared with the RSFs of Si.[1]

EXPERIMENTAL

All measurements were performed with a Cameca IMS-6f ion microprobe. We used both Cs^+ and O_2^+ primary ion beams for our analysis. During all measurements we used the most common mode for the large-area SIMS analysis with Cameca 4f-6f instruments:[2] so-called 'microscope mode' with a 150 μm field of view and an area of analysis of 60 μm diameter (contrast aperture of 150 μm and field aperture of 750 μm). For high mass resolution (HMR) mode we used a 400 μm contrast aperture. The energy window was kept fully open (energy bandpass ~130 eV) for the low mass resolution (LMR) mode ($M/\Delta M \sim 300$) and was closed down to 30–50 eV (dependent on the mass resolution power, MRP) for the HMR mode. The base pressure in the sample chamber was around 1×10^{-10} Torr. It increased to 4×10^{-10} Torr during analysis with the Cs^+ beam and to 6×10^{-10} Torr for O_2^+ beam analysis. The depth scale was calculated after measurement of the sputtering crater depth, performed with a Dektak profilometer. The experimental error of the measurements was ~4%.

The experimental samples that we used were 6H-SiC of orientation (0001) grown by CREE, Inc. The ion implantation was performed with an Ion-500 implanter (High Voltage Engineering Europe). A detailed description of implantation regimes, as well as experimental and theoretical projected ranges (R_p) calculated with the TRIM code (the stopping/range table) and taken from the literature,[3] are summarized in Table 1. The experimental R_p was taken as the depth of the distribution maximum. The RSFs were calculated using the doses of implantation, which were defined during implantation with an accuracy of ~5%.

RESULTS AND DISCUSSION

The data in Table 1 demonstrate good agreement between the theoretical and experimental R_p values. For both calculations the maximum deviation from experimental data does not exceed 15%. The sputtering yield for 6H-SiC was 1.6–2.0-fold less (depending on analysis conditions) than for Si under the same conditions.

Figure 1 demonstrates the depth profiles of H-, N-, O-, Be-, B- and Al-implanted SiC measured under 'optimal' conditions. 'Electronegative' elements (Fig. 1(a)) were measured under cesium ion sputtering and monitoring of secondary negative ions; 'electropositive' elements (Fig 1(b)) were analyzed under oxygen ion sputtering with monitoring of positive secondary ions. We also monitored the CsM^+ ion cluster (where M is the element of interest) under cesium

*Correspondence to: Yu. Kudriavtsev, Dep. Ingeniería Electrica-SEES, CINVESTAV-IPN, Av. IPN 2508, Col. San Pedro Zacatenco, México D.F. 07360, México.
E-mail: yuriyk@mail.cinvestav.mx
Contract/grant sponsor: CONACYT, Mexico; Contract/grant number: 31106.

Table 1. Description of the implanted standards: ion energy, ion dose and experimental and theoretical[2] projected ranges (R_p); density of SiC was chosen as 3.22 g cm^{-3} for TRIM calculations

Element	Energy (keV)	Dose (ions cm^{-2})	R_p, exp. (Å)	R_p[2] (Å)	R_p, TRIM (Å)
H	30	1.0×10^{15}	2600	2603	2371
B	90	1.0×10^{14}	1730	1767	1934
Be	40	3.2×10^{15}	1370	—	1237
O	90	1.0×10^{15}	1330	1432	1292
N	90	2.0×10^{14}	1670	—	1421
Al	100	2.0×10^{15}	950	900	1097

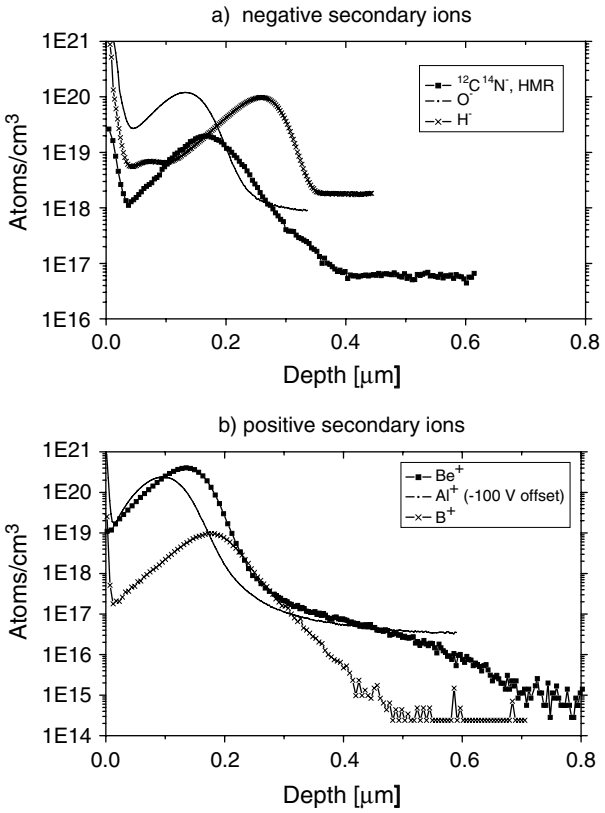

Figure 1. Depth profiles of implanted SiC standards measured under the 'optimal' SIMS conditions.

ion bombardment. Additionally, we utilized all possible secondary ions (atomic and cluster) that can be applied for the SIMS analysis.

Experimental RSFs for all regimes and for all analyzed atomic and cluster ions are shown in Tables 2(a)–2(c), together with the detection limits found for each regime. A good daily reproducibility of RSFs was found for all standards: the maximum deviation did not exceed 5%. In Table 3 we collected for comparison several SiC RSFs obtained in other studies[4,5] for some elements from our list, as well as for As and Ga, which are widely used for SiC doping.

We found that detection limits for B and Be in SiC are close to those for silicon. The fairly high level of volume concentration for the other gas elements (H, O, N) in comparison with silicon (see Fig. 1(a)) can be explained, in our opinion, by peculiarities in the SiC growth process. Note that the detection limit in all three cases corresponds to the bulk concentration of the analyzed element. In order to check this, we have compared them under different primary ion current densities: the same values were acquired.

We now consider some distinguishing features of the SIMS analysis of these elements in SiC.

Beryllium and boron

No important difference was noted between the analysis of Be and B implanted in SiC in comparison with silicon matrix.[1] Both elements can be analyzed effectively as negative as well as positive atomic ions; the positive secondary ions provide a more dynamic range. There is no mass interference, which if present could complicate analysis. Note that the CB^- ion signal provides another way for effective boron analysis with record sensitivity. The detection limit for both elements can reach 10^{14} atoms cm^{-3} (see Table 2(b)).

Aluminum

There is an interference between $Al^{\pm}$ and $C_xH_y^{\pm}$ clusters, which is more pronounced for negative secondary ions. There is also a memory effect if an Al/Cu grid is used for the instrument optics alignment. Sputtering of the sample will coat the surfaces that cause the memory effect. Applying a voltage offset of −100 V can reduce the mass interference. The HMR mode of $M/\Delta M = 1600$ can be utilized for effective analysis (see Table 2(b)) when the memory effect can be suppressed.

The experimental detection limit of Al in SiC was almost two orders of magnitude higher than in silicon[1] and corresponds to the bulk concentration of Al in the standard used. From our previous experience with other SiC samples, the detection limit of Al was $<10^{15}$ atoms cm^{-3}.[6]

Hydrogen

Again, there is no essential difference between analysis of H in SiC in comparison with Si matrix:[1] the negative atomic ion H^- yields the optimum sensitivity and detection limit. Note that the bulk concentration of H (as well as those of O and N) can depend on the SiC growth conditions. Some cluster ions such as $SiH^{\pm}$ and Cs_2H^+ can be utilized effectively. The latter cluster ion makes it possible to analyze hydrogen together with any 'electropositive' elements during one measurement.

Nitrogen

Nitrogen has a very high ionization potential (14.53 eV) and negative electron affinity. As a result, both positive and negative secondary ion yields of nitrogen ions are very poor or absent. In order to analyze N in silicon, the SiN^- cluster ion is commonly used.[1] For the SiC matrix there is a strong mass interference between the $^{28}Si^{14}N^-$ cluster ion and the $^{29}Si^{13}C^-$ cluster ion. To separate the interference it is necessary to apply a mass resolution power (MRP) of $M/\Delta M \sim 270\,000$, which is higher than the instrument permits.

We found that the $^{12}C^{14}N^-$ ion cluster, measured under HMR conditions with an MRP of $M/\Delta M \sim 7.500$, gives the highest sensitivity and the best detection limit (see Table 2(b)

Table 2(a). Experimental SiC RSFs and detection limits (DLs) for positive ions measured under O_2^+ primary ions sputtering with respect to Si; the last two columns show RSFs and DLs for Si[1]

	SiC		Si[1]	
Monitored ion	RSF (atoms cm^{-3})	DL (atoms cm^{-3})	RSF (atoms cm^{-3})	DL (atoms cm^{-3})
$^{1}H^{+}$	2.5×10^{24}	1.0×10^{19}	6.2×10^{24}	2.3×10^{18}
$^{28}Si^{1}H^{+}$	8.7×10^{24}	8.5×10^{18}	1.4×10^{25}	2.7×10^{18}
$^{9}Be^{+}$	3.1×10^{22}	1.0×10^{14}	3.2×10^{22}	4.7×10^{13}
$^{12}C^{11}Be^{+}$	5.8×10^{24}	8.0×10^{17}	—	—
$^{11}B^{+}$	5.6×10^{22}	1.0×10^{14}	6.5×10^{22}	1.8×10^{14}
$^{27}Al^{+}$ (HMR)[a]	1.5×10^{21}	3.0×10^{16}	1.4×10^{21}	7.0×10^{13}
$^{27}Al^{+}$ (−100 V offset)[b]	2.5×10^{23}	3.0×10^{16}	—	7.0×10^{13}
$^{27}Al^{12}C^{+}$[a]	3.5×10^{24}	1.4×10^{17}	—	—
$^{28}Si^{27}Al^{+}$[a]	7.5×10^{23}	4.2×10^{17}	4.8×10^{23}	7.0×10^{17}
$^{14}N^{+}$ (HMR)[c]	2.7×10^{24}	1.0×10^{17}	2.9×10^{25}	1.0×10^{19}

[a] HMR mode with $M/\Delta M \sim 2000$.
[b] The energy bandpass was ~60 eV.
[c] HMR mode with $M/\Delta M \sim 2500$.

Table 2(b). Experimental SiC RSFs and detection limits (DLs) for negative ions measured under Cs^{+} primary ions sputtering with respect to Si; the last two columns show RSFs and DLs for Si[1]

	SiC		Si[1]	
Monitored ion	RSF (atoms cm^{-3})	DL (atoms cm^{-3})	RSF (atoms cm^{-3})	DL (atoms cm^{-3})
$^{1}H^{-}$	4.2×10^{23}	1.7×10^{18}[a]	4.8×10^{23}	9.0×10^{16}
$^{30}Si^{1}H^{-}$	5.4×10^{24}	3.0×10^{18}	2.0×10^{24}	2.1×10^{17}
$^{9}Be^{-}$	9.2×10^{26}	5.2×10^{18}	2.0×10^{27}	—
$^{12}C^{9}Be^{-}$	1.3×10^{24}	2.8×10^{17}	—	—
$^{11}B^{-}$	1.9×10^{24}	4.7×10^{15}	2.4×10^{24}	2.2×10^{15}
$^{28}Si^{11}B^{-}$	9.4×10^{23}	1.7×10^{17}	—	3.6×10^{15}
$^{12}C^{11}B^{-}$	1.4×10^{23}	5×10^{14}	—	—
$^{16}O^{-}$	6.4×10^{22}	8.4×10^{17}[a]	2.4×10^{22}	8.0×10^{15}
$^{28}Si^{16}O^{-}$	7.9×10^{24}	1.7×10^{18}	1.0×10^{25}	—
$^{12}C^{14}N^{-}$ (HMR)[b]	4.9×10^{21}	5.4×10^{16}[a]	—	—
Al^{-} (HMR)[c]	6.9×10^{24}	1.8×10^{17}	1.2×10^{25}	1.0×10^{17}

[a] Bulk concentration.
[b] HMR mode with $M/\Delta M \sim 7500$.
[c] HMR mode with $M/\Delta M \sim 2000$.

Table 2(c). Experimental SiC RSFs and detection limits (DLs) for CsM^{+} ion clusters measured under Cs^{+} ion sputtering with respect to $^{133}Cs^{28}Si$; the last column shows RSFs for Si[1]

Monitored ion	RSF for SiC (atoms cm^{-3})	DL for SiC (atoms cm^{-3})	RSF for Si[1] (atoms cm^{-3})
$^{133}Cs_2^{1}H^{+}$	1.2×10^{22}	3.0×10^{18}	—
$^{133}Cs^{9}Be^{+}$	1.4×10^{22}	1.8×10^{17}	7.8×10^{21}[a]
$^{133}Cs^{11}B^{+}$	4.0×10^{22}	2.0×10^{17}	—
$^{11}B^{+}$	3.3×10^{22}	5.0×10^{16}	—
$^{133}Cs^{27}Al^{+}$	5.0×10^{21}	4.2×10^{17}	1.6×10^{21}[a]
$^{133}Cs^{28}Si^{16}O^{+}$	3.2×10^{21}	8.4×10^{18}	—
$^{133}Cs^{16}O^{+}$	1.5×10^{24}	1.7×10^{19}	1.4×10^{24}[a]
$^{133}Cs^{14}N^{+}$	6.5×10^{23}[a]	1.6×10^{17}	4.3×10^{23}[a]
$^{133}Cs_2^{14}N^{+}$	2.8×10^{23}[a]	8.8×10^{16}	—

[a] With respect to Si. Multiply RSF values by 2.2 to compare with CsSi reference.

Table 3. The SiC RSFs and detection limits (DLs) for a set of elements taken from the literature[4,5]

Element	Monitored ion	Reference ion	RSF (atoms cm^{-3})	DL (atoms cm^{-3})
H	$^{1}H^{-}$	$^{28}Si^{-}$	3.0×10^{23}	8.0×10^{17}
H	$^{133}Cs_2^{1}H^{+}$	$^{133}Cs_2^{28}Si^{+}$	1.1×10^{22}	
B	$^{11}B^{+}$	$^{28}Si^{+}$	4.0×10^{22}	1.0×10^{14}
B	$^{133}Cs^{11}B^{+}$	$^{133}Cs^{28}Si^{+}$	4.5×10^{22}	
B	$^{133}Cs_2^{11}B^{+}$	$^{133}Cs_2^{28}Si^{+}$	1.8×10^{23}	
N	$^{133}Cs^{14}N^{+}$	$^{133}Cs^{28}Si^{+}$	1.8×10^{23}	
Al	$^{133}Cs^{75}Al^{+}$	$^{133}Cs^{28}Si^{+}$	4.5×10^{21}	
Al	$^{27}Al^{+}$	$^{28}Si^{+}$	5.0×10^{21}	1.0×10^{15}
Ga	$^{133}Cs^{69}Ga^{+}$	$^{133}Cs^{28}Si^{+}$	2.5×10^{21}	
Ga	$^{71}Ga^{+}$	$^{28}Si^{+}$	1.0×10^{22}	5.0×10^{14}
As	$^{133}Cs^{75}As^{+}$	$^{133}Cs^{28}Si^{+}$	2.6×10^{22}	

and Figs 1(a) and 2(b)). If necessary, the HMR mode can be used for monitoring N^+ secondary ions. An MRP of $M/\Delta M \sim 2.500$ is enough to separate $^{28}Si^{2+}$, $^{14}N^+$ and $^{13}C^1H^+$ secondary ions (Fig. 2(a)) but, as noticed before, the N^+ ion intensity is quite low (see Table 2(a)). The CsM^+ mode also can be utilized. Note that the Cs_2N^+ cluster ion current gives a more dynamic range for nitrogen analysis compared with CsN^+ ions.

The detection limit of nitrogen in SiC is under question. Our standard has a bulk concentration of nitrogen equal to 5.4×10^{16} atoms cm^{-3}. From the HMR spectrum (Fig. 2(a)), measured far from the implanted maximum we can estimate a nitrogen detection limit as low as 5×10^{14} atoms cm^{-3} with the vacuum in the sample chamber $<5 \times 10^{-10}$ Torr.

Oxygen

The O^- ion represents the best dynamic range of oxygen analysis (see Table 2(b)) in SiC. Utilization of the $CsSiO^+$ ion cluster can be a good choice because of its high intensity and the possibility of simultaneous analysis of electropositive and electronegative elements in this case.

During negative SIMS analysis of oxygen we found a difference in the oxygen distribution measured with SiO^- ions in comparison with O^- ions (see Fig. 3). We exclude any apparatus and depth calculation effects by having simultaneous measurement for both ions. There was no charging during the measurement. Moreover, there was no similar behavior for other elements under the same conditions.

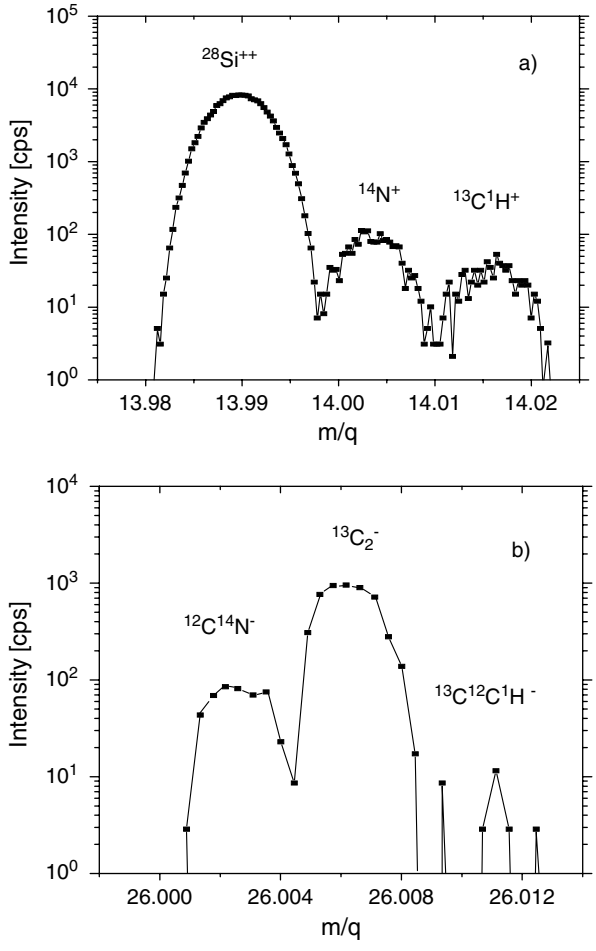

Figure 2. High mass resolution spectra obtained for nitrogen-implanted SiC in both 'positive' (a) and 'negative' (b) secondary ion modes.

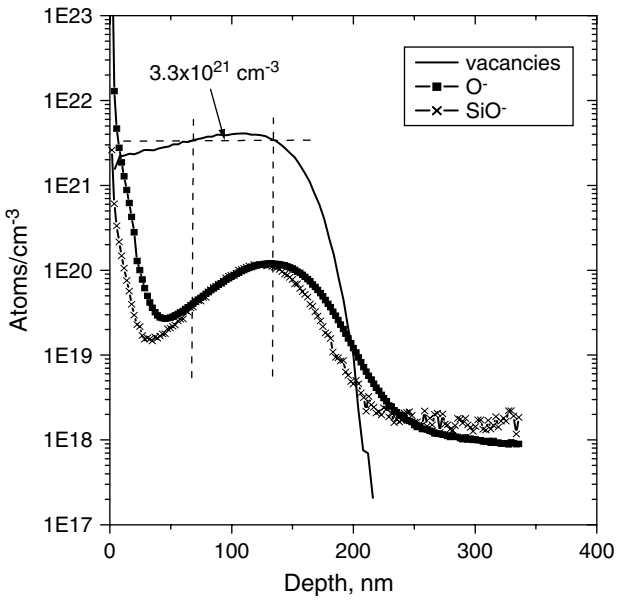

Figure 3. The SIMS depth profile of oxygen-implanted SiC acquired with O^- and SiO^- secondary ions. The vacancy distribution calculated using TRIM is presented for comparison. (For details, see text.)

In order to explain the effect, we considered SiO^- ion cluster formation carefully. The cluster formation was separated into two steps: SiO molecule formation on the surface with subsequent emission (Direct Emission model[7] of sputtered clusters); and ionization of the cluster after removal from the surface. We assume the same ionization probability of SiO clusters during all depth profiling except the surface maximum, which is defined by the transient effect. Thus, the difference in O^- and SiO^- ion yields should be explained by a different probability of SiO formation for different depths. To understand this, we performed a computer simulation of the oxygen implantation in SiC with the Monte-Carlo computer code TRIM. We analyzed the distribution of vacancies formed during implantation, which correlates with an energy transfer between implanting ions and atoms of the solid (see Fig. 3). From a comparison of the SiO^- and O^- distributions we found that agreement between them is observed for a small part of the profiles, which correlates with the maximum of the vacancies distribution. A more careful study gives us the 'threshold' number of vacancies of $\sim 3.3 \times 10^{21}$ cm^{-3} (see Fig. 3). This value is almost 3% of the total atomic concentration in SiC. There is a strong correlation between the vacancy formation and the energy loss of the primary ion due to its collision with solid atoms. Thus, we can estimate the existence of a 'threshold' energy required to break Si–C bonds. After the 'energy threshold' is exceeded, most of the Si–C bonds are broken and very strong Si–O bonds (which are stronger than Si–C bonds) are formed. Before that, the strong Si–C bonds partly prevented Si–O formation. Thus, the different degree of amorphization of SiC, depending on the depth, caused by

the ion implantation explains the different probability of SiO molecule formation during SIMS depth profiling analysis. In such a manner, SiO^- cluster ions cannot represent the oxygen distribution correctly.

Matrix effect

In Tables 2(a)–2(c) we have presented the RSFs for silicon obtained under similar conditions.[1] From a comparison of the data we can conclude a minor matrix effect for most of the elements when the measurements are performed for atomic ions and for CsM^+ cluster ions. In the case of other clusters, as well as for the HMR mode, the matrix effect becomes essential. We estimate that a fine instrument alignment, which varies for different instruments, together with a modification of the cluster formation process in SiC found for SiO, yields the observed RSF difference.

CONCLUSION

The experimental RSFs for the SIMS analysis of 6H-SiC were found for various SIMS regimes. A matrix effect (in comparison with silicon) was observed only for cluster ions (except for CsM^+ clusters) and in the case of the HMR mode. The detection limit of some analyzed elements for SiC was determined to be 1.5–2.0-fold less than for Si, which correlates with the sputtering yield difference found for these matrixes.

The SIMS depth profiling analysis of SiC with cluster ions can lead to errors in some cases.

Acknowledgement

The authors from CINVESTAV thank CONACYT (Mexico) for financial support of this work under grant no. 31106.

REFERENCES

1. Wilson RG, Stevie FA, Magee CW. *Secondary Ion Mass Spectrometry. A Practical Handbook for Depth Profiling and Bulk Impurity Analysis*. John Wiley: Chichester, 1989; p. 543.
2. *IMS-6f User's Guide*. Cameca: France; 1995.
3. Burenkov AF, Komarov FF, Kumakhov MA, Temkin MM. *Tables of spatial distribution of ion-implanted dopant*. Minsk: Byelarussian State University, 1980 (In Russian).
4. Linnarsson MK, Svensson BG. In *Proceedings of Tenth International Conference on Secondary Ion Mass Spectrometry, SIMS X*, Benninghoven A, Hagenhoff B (eds). John Wiley: Chichester, 1997; pp. 553–556.
5. Marie Y, Bieck W, Migeon H-M. *Proceedings of Tenth International Conference on Secondary Ion Mass Spectrometry, SIMS X*, Benninghoven A, Hagenhoff B (eds). John Wiley: Chichester, 1997; pp. 685–688.
6. Usov IO, Suvorova AA, Sokolov VV, Kudriavtsev YA, Suvorov AV. *J. Appl. Phys.* 1999; **86**: 6039.
7. Gerhard W, Oechsner H. *Z. Phys. B.* 1975; **22**: 41.